



# Circumpolar projections of Antarctic krill growth potential

Devi Veytia<sup>1</sup>✉, Stuart Corney<sup>1</sup>, Klaus M. Meiners<sup>2,3</sup>, So Kawaguchi<sup>1,2,3</sup>, Eugene J. Murphy<sup>1,4</sup> and Sophie Bestley<sup>1,3</sup>

**Antarctic krill is a key species of important Southern Ocean food webs, yet how changes in ocean temperature and primary production may impact their habitat quality remains poorly understood. We provide a circumpolar assessment of the robustness of krill growth habitat to climate change by coupling an empirical krill growth model with projections from a weighted subset of IPCC Earth system models. We find that 85% of the study area experienced only a moderate change in relative gross growth potential ( $\pm 20\%$ ) by 2100. However, a temporal shift in seasonal timings of habitat quality may cause disjunctions between krill's biological timings and the future environment. Regions likely to experience habitat quality decline or retreat are concentrated near the northern limits of krill distribution and in the Amundsen–Bellingshausen seas region during autumn, meaning habitat will likely shift to higher latitudes in these areas.**

**A**ntarctic krill (*Euphausia superba*, hereafter krill) are an ecologically<sup>1–4</sup> and commercially<sup>5,6</sup> important species in the Southern Ocean, and yet qualitative reviews hypothesize that krill may be vulnerable to projected oceanic warming as stenothermic crustaceans<sup>7–9</sup>. Previous projections have suggested that ocean warming will cause favourable krill habitat to contract<sup>10,11</sup>, resulting in possible declines in abundance and/or biomass. Currently, oceanic warming is manifesting more rapidly in regions of the Southern Ocean than the global average<sup>12,13</sup>, but its effect on observed krill abundance and distribution is a topic of debate<sup>14–18</sup>. Predicting the population response of krill to climate change, and the ecological impacts of these changes, is therefore important to conservation efforts and the management of the krill fishery<sup>8</sup>.

Projecting future changes in krill habitat requires knowledge of environmental drivers of habitat quality. Existing empirically based models describe krill growth as a function of two major factors: temperature and food concentration (typically phytoplankton approximated by primary production (PP) and/or chlorophyll *a*)<sup>19–21</sup>. Thus, accurate estimates of these variables are required. Recent advances in computing capacities now allow climate models to support the reasonable representation of the carbon cycle within fully coupled Earth system models (ESMs)<sup>22</sup>. However, it remains difficult for modelled PP fields to reproduce current observations with a resolution and accuracy sufficient for application to biological models<sup>23,24</sup>.

Existing studies modelling future changes in krill habitat have so far explored future PP by manipulating (that is, % increase/decrease) satellite chlorophyll *a* observations. For example, projected changes in sea surface temperature (SST) and sea ice resulted in changes in spawning habitat ranging from +51% to –83%, depending on changes in summer chlorophyll *a* of +25% to –50%<sup>25</sup>. Increases in SST also resulted in mid-latitude (~55–65°S) declines in adult krill habitat quality, and potentially biomass<sup>10,11</sup>, although these declines could be partially mitigated by a 50% increase in chlorophyll *a*<sup>10</sup>. A wider analysis of Southern Ocean PP from the Coupled Model Intercomparison Project 5 (CMIP5) ensemble suggests this mitigating interaction to be unlikely, reporting a latitudinally banded

response to climate change with reduced PP in mid-latitude regions<sup>26</sup>. Further studies<sup>27–30</sup> indicate that future changes in the timing of seasonal PP may result in a temporal mismatch between the seasonal cycle of krill and food availability. Krill habitat is therefore highly sensitive to future changes in PP, for which skilled model projections are needed<sup>11</sup>.

We combine projections of both SST and chlorophyll *a* to provide simulations of circumpolar krill growth potential as a measure of adult krill habitat quality. To calculate growth potential, we built on an existing method<sup>11</sup>, forcing an empirical growth model<sup>21</sup> for a 40 mm krill with projected seasonal climatologies for 2070–2099 from an ensemble of ESMs. To improve the ESM ensemble performance for biological modelling applications, we developed an approach to select and weight ESMs on the basis of their skill at reproducing observation-based growth potential for the recent past. Projections from the weighted subset are presented for two representative concentration pathways (RCPs): RCP 4.5 and RCP 8.5. Relative gross growth potential (RGGP) projections are developed using a krill length/mass relationship<sup>10,31,32</sup>.

**Evaluation of ESM selection and weighting approach.** Assuming model biases remain consistent with time, selecting ESMs that most accurately reproduce current climate can increase confidence in future projections<sup>33</sup>. Yet reducing the number of models contributing to a projection can limit predictive power. Of 11 CMIP5 ESMs that contributed chlorophyll *a* and SST for the relevant RCP scenarios, most produced seasonal SST climatologies for the historical period (1960–1989) that closely matched Southern Ocean observations (Extended Data Figs. 1 and 2). The observed variability in chlorophyll *a* was typically misrepresented by relatively simple biogeochemical models with high intermodel variation (standard deviation axes, Extended Data Fig. 2). Since the krill growth model is highly sensitive to changes in chlorophyll *a*<sup>11</sup>, spatial variability was also typically misrepresented in growth potential (Fig. 1).

Our selection and weighting approach (see Methods) ensured that modelled growth potential more closely matched

<sup>1</sup>Institute for Marine and Antarctic Studies, University of Tasmania, Hobart, Tasmania, Australia. <sup>2</sup>Australian Antarctic Division, Department of Agriculture, Water and the Environment, Kingston, Tasmania, Australia. <sup>3</sup>Antarctic Climate and Ecosystems Cooperative Research Centre, University of Tasmania, Hobart, Tasmania, Australia. <sup>4</sup>British Antarctic Survey, Cambridge, UK. ✉e-mail: Devi.Veytia@utas.edu.au

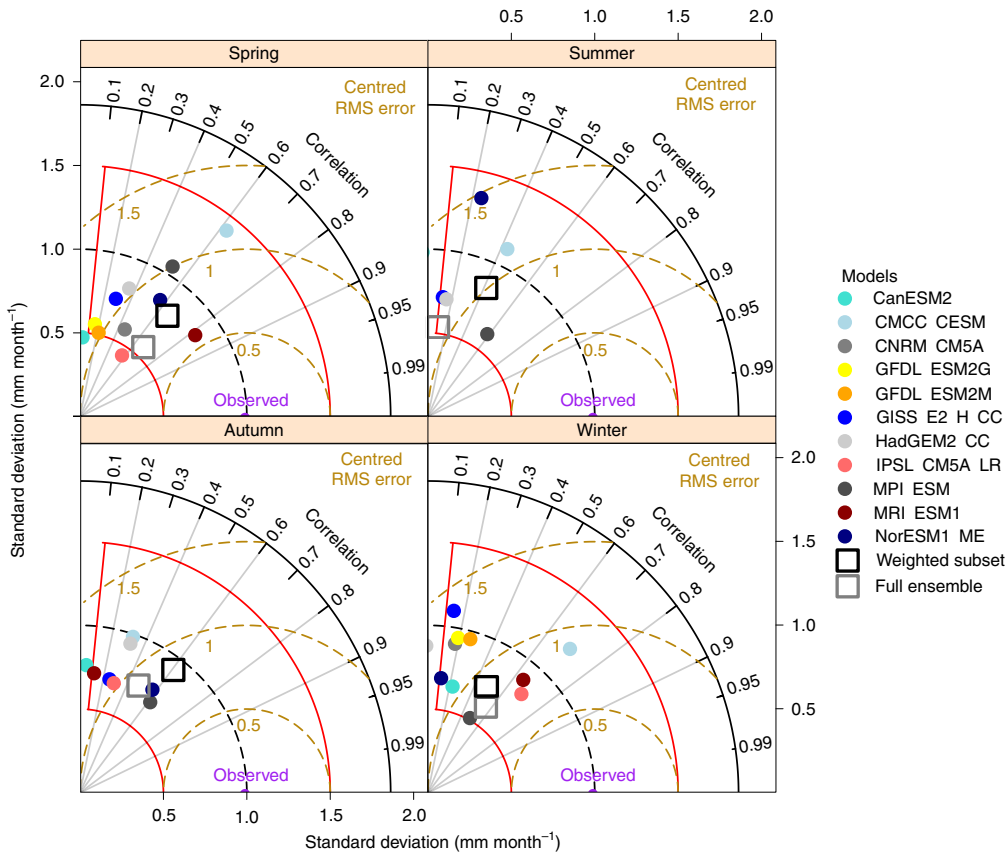


**Fig. 1 | Taylor diagram assessing individual model performance in projecting growth potential against observation-based values for selection and weighting scheme.** Available models in the full ensemble are plotted with circles, while the weighted subset and unweighted full ensemble mean are plotted in squares. Models not pictured have negative correlation and are outside the plotting range. Statistics for the Taylor diagram were calculated from the area-weighted seasonal surface averages of growth potential. Observation-based growth potential was calculated using the average of the Sea-viewing Wide Field-of-View Sensor (SeaWiFS)<sup>75</sup> and Johnson et al.<sup>76</sup> chlorophyll datasets. For each season, models that fell outside the red line boundary were not included in the weighting scheme. Weighting was then assigned on the basis of weighting scheme 4 (see Methods and Supplementary Table 2).

observation-based variability than did using the full ensemble mean (Fig. 1). Across all seasons, the weighted subset growth potential shows normalized root mean square errors between 0.75 and 1 (0.6–1.2 for the full ensemble), correlation coefficients between 0.4 and 0.7 (0.1–0.7) and normalized standard deviations within  $\pm 0.7$  ( $\pm 0.9$ ) of observation-based growth potential. The models displayed seasonal variation in their skill, which was reflected in the seasonal differences of the weightings (Supplementary Table 2).

Our weighting approach had the largest effect on chlorophyll *a*, first because there was higher intermodel variation in chlorophyll *a* estimates. Second, the weighting acted largely on growth potential variability, which originated primarily from variability in chlorophyll *a* due to the growth model sensitivity. A previous analysis<sup>26</sup> projected changes in maximum annual surface phytoplankton under RCP 8.5, calculated for the CMIP5 multimodel mean. Here, using seasonal chlorophyll *a* calculated for the weighted ensemble mean, we see evidence of at least two latitudinal bands of change under RCP 4.5 (spring) and RCP 8.5 (spring–summer), consistent with this previous finding (Fig. 2b). However, our weighted subset projected localized decreases in chlorophyll *a* over the continental shelf in summer and generally more zonal structuring in the manifested change.

Seasonal growth potential maps confirmed that, by prioritizing variability, the weighted approach reproduced the observation-based growth potential with improved magnitude and distribution relative to the full ensemble (Fig. 3). There were several regions that deviated

from observation-based values. Regions of expected limited growth upstream of the Kerguelen Plateau and in the Amundsen Sea were not as well resolved. In autumn, localized regions of growth potential  $>4\text{ mm month}^{-1}$  were underestimated, leading to an underestimation in spatial variability. This was probably due to few models receiving high weighting in this season (Supplementary Table 2). In addition, known model biases in SST and sea ice result in growth areas extending into higher latitudes than observed in winter and spring<sup>34</sup>.

**Projected krill habitat quality shifts in space and time.** Projected changes in krill habitat quality (growth potential) and habitat area (the total area where growth potential was positive) were evaluated between the recent past (1960–1989) and end of the century (2070–2099) (Fig. 4 and Supplementary Figs. 4 and 5). The major projected changes in growth potential reflect the projections of the future environmental drivers (projected SST and chlorophyll *a*; Fig. 2). As with the historical climatology, future projections display seasonal variation, but seasonal differences between RCP scenarios were relatively minor. In spring, summer and winter, RCP 8.5 resulted in slightly lower median growth potential than RCP 4.5 (Table 1). This was due to an increase in SST and slight decline in chlorophyll *a* in summer. Due to seasonal similarities, the results of the two RCP scenarios are presented together.

Krill habitat quality is expected to improve in spring. Growth potential increased south of  $60^{\circ}\text{S}$ . Habitat area increased by 13% and 10% under RCP 4.5 and 8.5, respectively; the regions of krill habitat

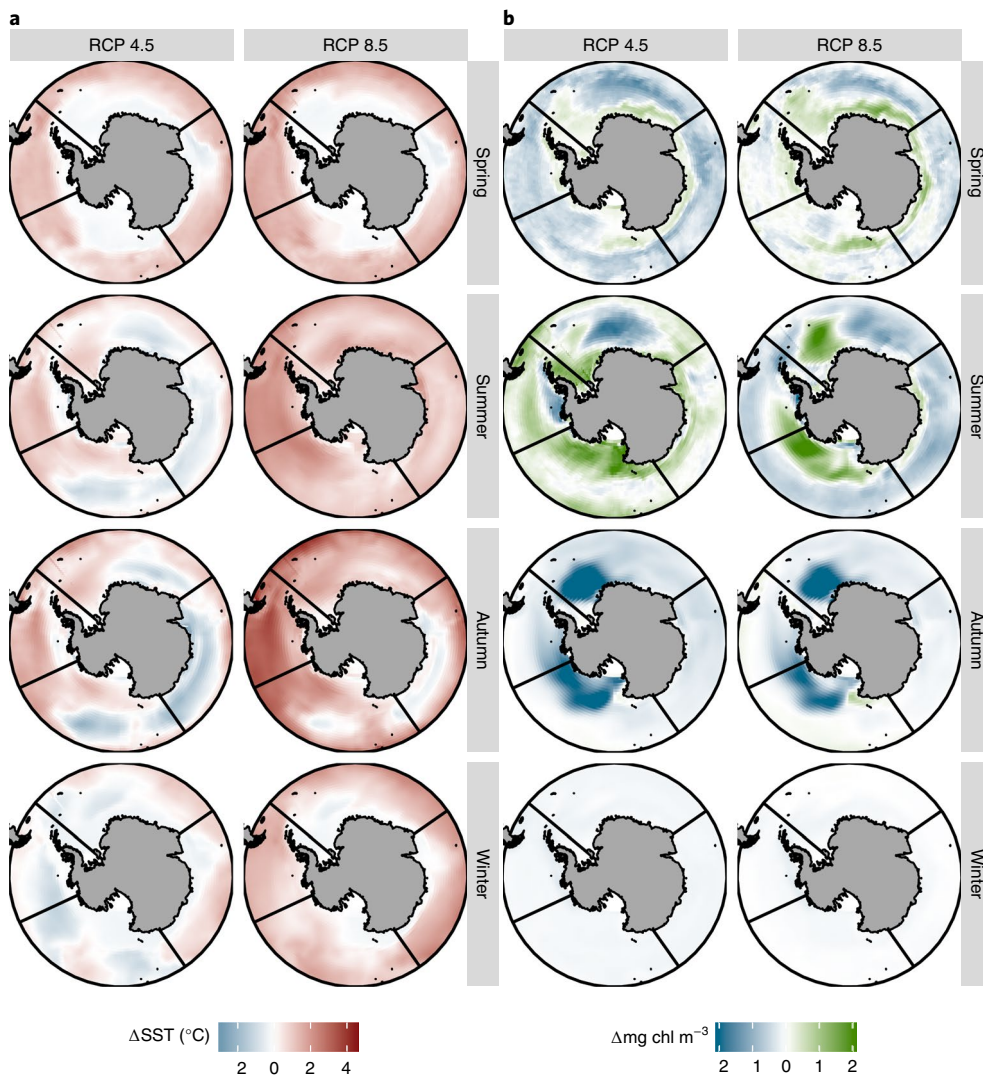


**Fig. 2 | Changes in future environmental drivers projected by the weighted subset for RCP scenarios 4.5 and 8.5. a, SST. b, Chlorophyll *a* (chl).** Change is defined as the projected climatology minus the historical. Black meridional lines on maps delineate ocean basin sectors<sup>9</sup>.

expansion were concentrated on the continental shelf. This encroachment should be considered alongside the known low-sea-ice bias in spring<sup>34</sup>, which causes historical growth potential to extend farther south than observed. This bias will likely propagate into future projections, meaning habitat may not extend as far south as projected. While changes in krill habitat generally varied by latitude, there were regional exceptions of increased growth: to the east of and including the Weddell Sea under RCP 4.5 and the high latitude regions of the Bellingshausen and Amundsen seas under RCP 8.5.

In summer, there was an increase in habitat quality at high and low latitudes and a decline in the mid-latitudes. Results for summer are the most robust, as the empirical growth model was validated with summertime in situ data. The net circumpolar effect of these changes on habitat area resulted in a negligible increase under RCP 4.5 (+2%) and decrease under RCP 8.5 (-1%). Notably, the Antarctic Peninsula (AP), a potential source population<sup>35</sup> for the Scotia Sea downstream, is in the mid-latitude band of habitat quality decline, consistent with the banding pattern of changes in chlorophyll *a*. Regions of increased summer habitat quality include the eastern Weddell (15–45° W, RCP 4.5) and western Ross seas (160–180° E, RCP 4.5 and 8.5). Yet the Ross Sea is difficult to accurately depict in ESMs<sup>34</sup>, making projections there less certain.

Autumn displayed the greatest decline in habitat quality and area, especially under RCP 4.5. This constituted the greatest difference between the RCP projections but was probably due to a difference in model weighting rather than differences between the RCP scenarios themselves. One of the best-performing (thus highly weighted) models in autumn for the recent past (CMCC-Carbon Earth System Model (CMCC-CESM)) did not contribute RCP 4.5 projections to the CMIP5 archive. This suggests that our RCP 8.5 autumn projection is more reliable. Autumn decreases in growth potential and habitat area (-28% under RCP 4.5, -19% under RCP 8.5) occurred mainly in sub-Antarctic regions, including the eastern and central Pacific Ocean. These range contractions are attributed to warming SST (Fig. 2).

Finally, in winter, small declines in already low growth potential are projected at low latitudes due to warming SST while chlorophyll *a* remains low. The net impact of these changes on habitat area is negligible for RCP 4.5 (-3%) and results in a decline in RCP 8.5 (-10%).

In summary, projected krill habitat quality shifts towards higher latitudes due mainly to rising SST. Habitat quality also shifts temporally as a function of changing SST and chlorophyll *a* by improving in spring, declining in ecologically important regions

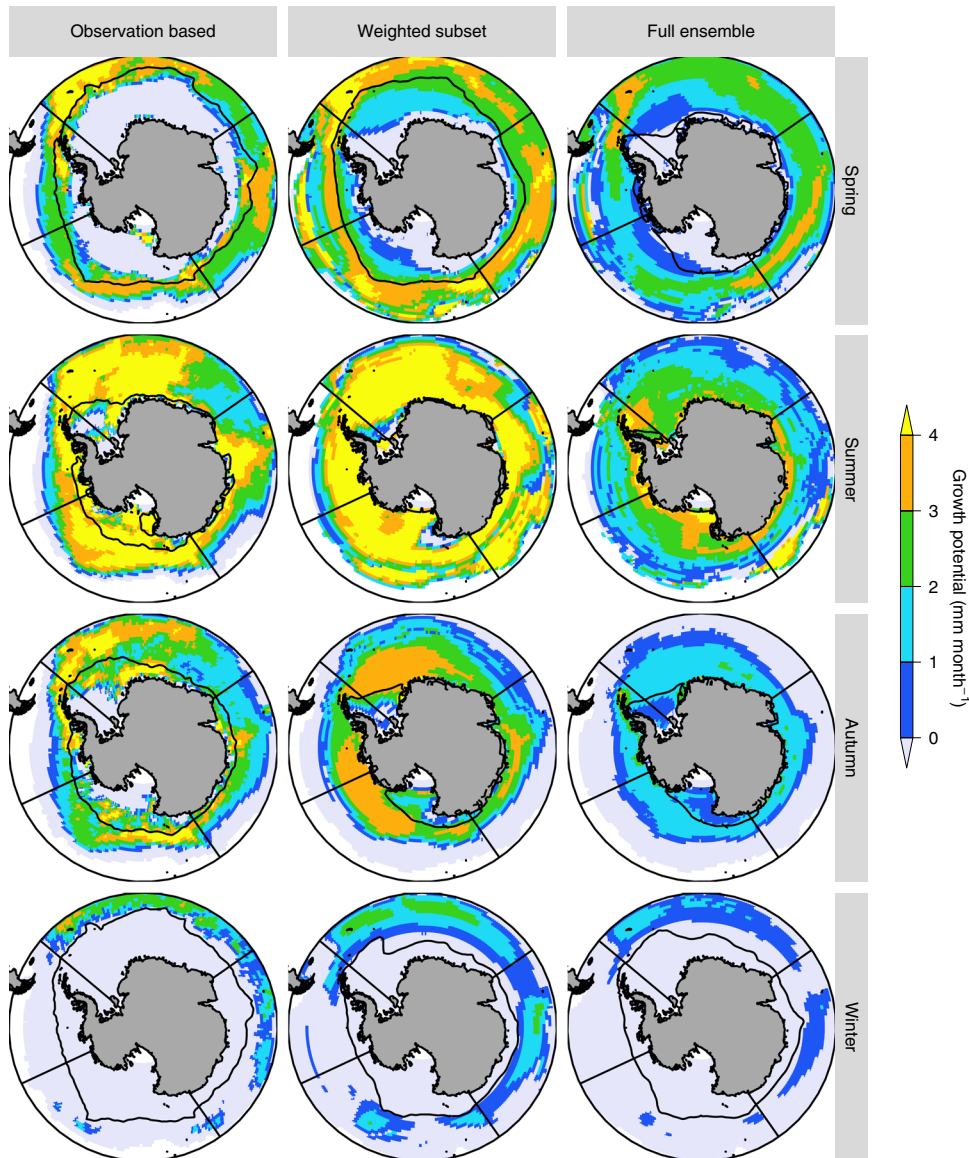


**Fig. 3 | Evaluating the performance of the weighted subset.** Mean growth potential calculated using seasonal averages (columns left to right) satellite observation datasets binned to the same  $1^\circ \times 1^\circ$  grid as the ESMs (chlorophyll was the mean between SeaWiFS<sup>75</sup> and Johnson et al.<sup>76</sup> datasets), the weighted multimodel mean of the model subset and the unweighted mean of the full ensemble. The seasonal climatologies were averaged from 1997 to 2010 for observation data and from 1960 to 1989 (the ‘historical’ period) for CMIP5 climate models. The black contour delineates where  $\text{SST} = -1^\circ\text{C}$ , below which the empirical krill growth model<sup>[2]</sup> has not been validated with in situ data and therefore represents extrapolation. Black meridional lines on maps delineate ocean basin sectors<sup>9</sup>.

in summer and declining overall in autumn. Projected circum-polar changes in habitat area are relatively small but positive in spring.

**Management implications.** The results of this study are relevant for future perspectives on krill fishery management, which is overseen by the Commission for the Conservation of Antarctic Marine Living Resources (CCAMLR). The krill fishery is the largest in the Southern Ocean, and its management is subdivided into statistical subareas<sup>5</sup>. Here we present results of RGGP—a habitat quality metric based on biomass rather than length<sup>10,31,32</sup>—and its environmental drivers (Supplementary Tables 3 and 4). Overall, 90% of CCAMLR subareas evaluated experienced a change in RGGP of less than 15% (Fig. 5). This comprises subareas south of the Southern Antarctic Circumpolar Current Front (SACCF) but including South Georgia (Subarea 48.3). The SACCF generally represents the northern limit of krill

distribution, except for South Georgia, which represents the upper limits of krill thermotolerance ( $\sim 4^\circ\text{C}$ )<sup>35,36</sup>.

Across all seasons, 40% of CCAMLR subareas projected increases in RGGP. Most of these are attributed to SST increases in spring, changing historically cold areas to temperatures more favourable for high growth. The three areas of greatest RGGP increase all demonstrate large increases in chlorophyll *a* (+25–175%), with only minor changes in SST (within  $0.1^\circ\text{C}$ ). Therefore, RGGP is projected to improve when changes in SST either are small and accompanied by increases in chlorophyll *a* or beneficially increase historically low temperatures in spring.

Krill are most sensitive to changes in temperature at the upper limits of their thermotolerance<sup>1,21</sup>; hence, areas exhibiting RGGP declines in excess of 20% were almost exclusively towards the northern limits of krill distribution. Declines in most of these regions were still relatively moderate; for example, during autumn

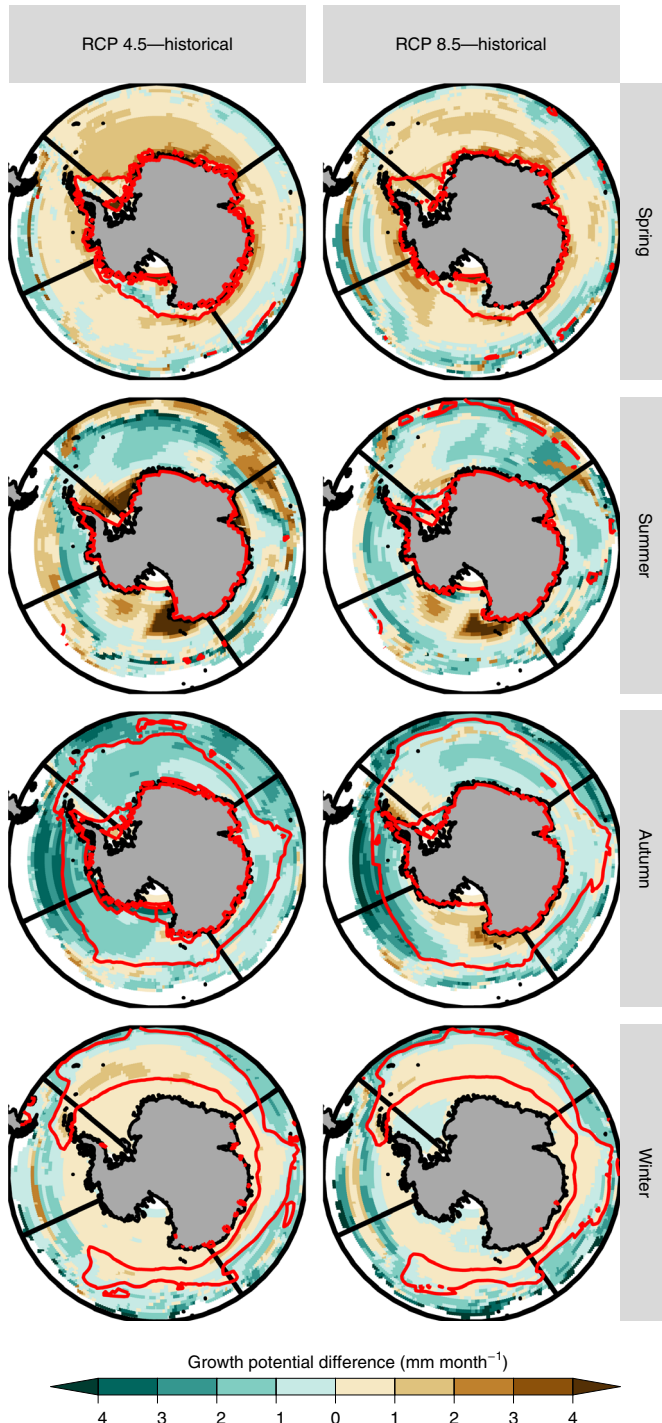


**Fig. 4 | The projected change in krill growth potential between each RCP scenario and the historical scenario.** The red contour delineates regions where growth potential is positive for each RCP projection. Note that in summer the red contour hugs the coastline, indicating the entire Southern Ocean exhibits growth in all situations. These projections represent the weighted subset mean. Black meridional lines on maps delineate ocean basin sectors<sup>9</sup>.

under RCP 4.5 in the Bellingshausen Sea (Subarea 88.3,  $-21\%$ ) and during summer under RCP 8.5 around South Georgia ( $-23\%$ ). These RGGP declines had different environmental drivers, with a decrease in chlorophyll *a* ( $-50\%$ ) and increase in SST ( $+1.7^{\circ}\text{C}$ ), and an increase in SST ( $+1.8^{\circ}\text{C}$ ), respectively.

**Table 1 | Median growth potential and model projection envelope**

Growth potential (mm month <sup>-1</sup> )	Spring	Summer	Autumn	Winter
Historical	2.00 (-1.12 to 5.64)	3.87 (3.83 to 5.44)	1.30 (0.36 to 2.89)	-1.14 (-2.07 to 0.68)
RCP 4.5	2.84 (0.36 to 5.58)	3.94 (3.77 to 5.19)	-0.20 <sup>a</sup> (-0.42 to 1.14)	-1.02 (-1.58 to 0.64)
RCP 8.5	2.24 (-0.40 to 5.65)	3.45 (3.35 to 5.09)	0.67 (0.16 to 2.08)	-1.35 (-2.02 to -0.43)

<sup>a</sup>One of the highest weighted models for this season did not contribute to the CMIP5 RCP 4.5 scenario (Supplementary Table 2). Therefore, the median projection is not consistent with those of the other two scenarios as the underlying weighting mechanism is vastly different. Values represent the median of all grid-cell growth potential values from the weighted subset mean, for each season and CMIP scenario. The analogous medians from the weighted subset 10% and 90% quantiles are shown in parentheses to illustrate the envelope of the projections (see Supplementary Appendix B for an explanation of the projection envelope and its associated Supplementary Figs. 1–3 for spatial patterning).

## Discussion

Refining an ESM ensemble in a new way allows the circumpolar projection of krill habitat quality. We found a temporal shift of habitat quality in the Antarctic Peninsula, with habitat improving in spring and declining in summer and autumn. This could have important implications for krill reproduction and population size as the tip of the AP is both an important spawning ground for krill within the Southwest Atlantic sector<sup>37</sup> and a major fishing ground for krill<sup>35</sup>.

Temporal shifts could influence krill population dynamics by offsetting the synchronization of krill life history to the annual cycle of the Antarctic environment<sup>11,30</sup>. In a stable climate, synchronization allows krill to efficiently use seasonally available food sources that facilitate growth, reproduction and overwintering<sup>38</sup>. A temporal shift in habitat quality could therefore create a timing mismatch. In this same AP region, modelling showed spawning habitat to be highly affected by future changes in the timing of sea-ice advance<sup>25</sup>. Furthermore, recent laboratory work suggests that krill lack the plasticity to adapt to temporal shifts as the seasonal physiological cycle of krill is entrained by light regime<sup>38,29</sup>.

In a typical reproductive season, food in late winter to early spring is important to allow krill to prepare for reproduction, while PP during summer is critical for completion of the reproductive cycle<sup>38</sup>. Our projections show that while krill may have a good start to maturation early in the season, the subsequent decline in habitat condition may negatively affect reproductive performance due to the exponential relationship between adult size and fecundity<sup>35,39</sup>. Decreases in projected summer growth potential around the AP ( $-1$  to  $-2 \text{ mm month}^{-1}$ ,  $-3$  to  $-6 \text{ mm month}^{-1}$  over the season) would translate into an exponential decrease in regional fecundity.

We also found a spatial shift in habitat quality towards higher latitudes. Northern regions where temperature increases begin to exceed krill thermotolerance<sup>11,21</sup> also showed associated decreases in projected chlorophyll *a*; the exception being South Georgia during summer under RCP 4.5. Previous regional-scale modelling work<sup>10</sup> hypothesized that increases in ocean PP might mitigate the increased physiological consequences of rising SST for krill. Our results suggest that projected changes in chlorophyll *a* and SST will more likely have a negative synergistic effect in low latitudes, while beneficial increases in chlorophyll *a* and SST in high latitudes may have a positive synergistic effect for krill growth.

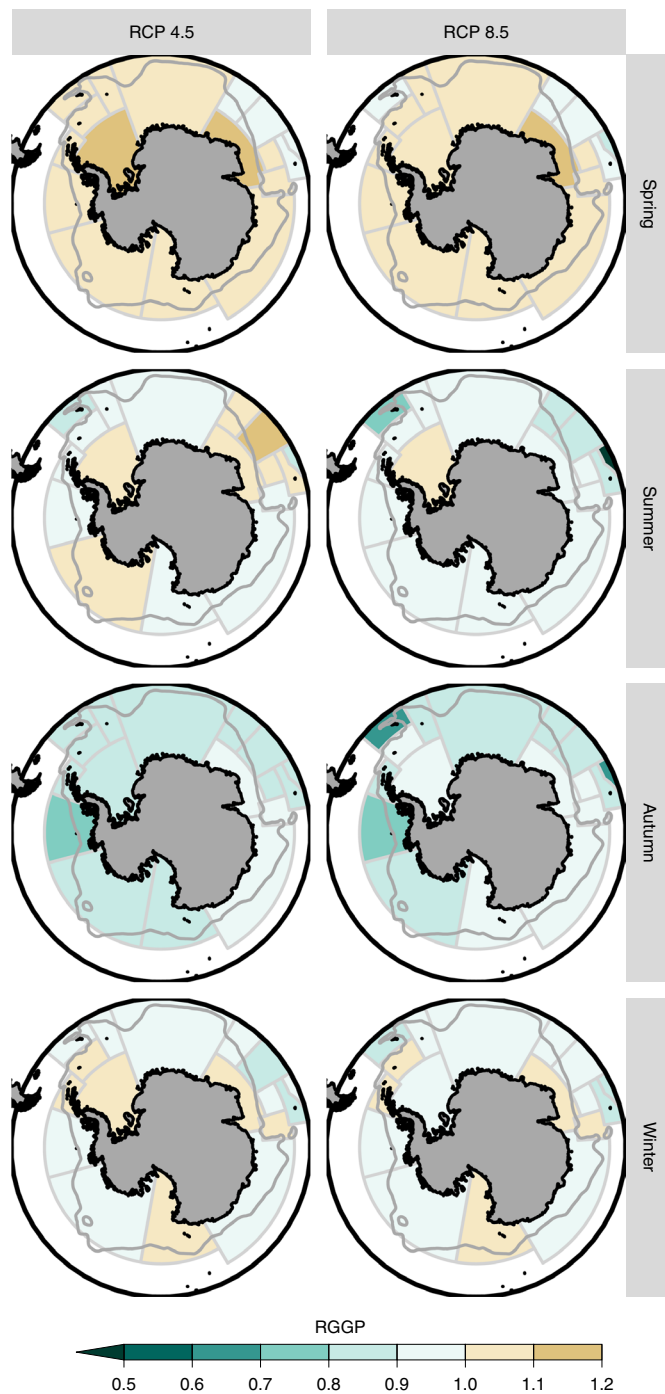


**Fig. 5 | The projected RGGP in CCAMLR management areas.** ‘Relative’ refers to the ratio between each RCP scenario and the historical scenario. The dark grey contour represents the location of the SACC<sup>27</sup>, which with the exception of South Georgia marks the northern boundary for krill distribution<sup>35</sup>. The contour for the SACC<sup>27</sup> was accessed using the `raadtools`<sup>78</sup> package.

Particularly high krill growth potential increases were projected for the eastern Weddell and western Ross seas in summer, which we have placed within the context of large-scale climate processes altering two major growth drivers (SST and chlorophyll *a*). However, regional-scale hydrographic features, such as the Antarctic Slope Current<sup>40</sup> and Ross Gyre<sup>41</sup>, are likely to have significant implications for habitat quality and growth potential; for example, variability in the strength of the Antarctic Slope Current between years and

the associated influx of Circumpolar Deep Water. Antarctic shelf and along-shelf processes are generally not well represented in the coarse grid scales of CMIP5 models<sup>40,42,43</sup>, but this will probably improve with future simulations undertaken on finer-scale grids.

Similarly, our results compile seasonal climatologies; however, the Southern Annular Mode (SAM) and the El Niño Southern Oscillation (ENSO) are known drivers of interannual variability in physical processes likely to impact krill growth potential<sup>15</sup>. Observational studies have linked positive SAM and strong ENSO events with decreases in krill density and recruitment, hypothesizing that these events degraded the quality of sea-ice habitat for overwintering krill<sup>15,17,44,45</sup>. Under anthropogenic forcing, CMIP5 models generally project an increasingly positive SAM<sup>46</sup> and possibly more El Niño events<sup>47</sup>. Therefore, a consideration of modes of climactic variability (ENSO and SAM), and their role in hydrographic and sea-ice variability, is needed to obtain more confident projections of krill habitat in these regions<sup>1,48</sup>.

Food availability (represented by chlorophyll *a*) is a primary driver of krill distribution and growth<sup>11,19,21</sup>. The chlorophyll *a* projections obtained using our weighted subset approach present broad-scale similarities, but some key regional differentiation, with those using an unweighted ensemble mean<sup>26</sup>. Our findings indicate the unweighted mean underrepresents historical growth potential (and chlorophyll *a*). Consequently, the weighting approach adopted here improves our confidence for this biological application. Overall, a central message across studies is that PP projections show important seasonal variability in responses to future change.

Our results suggest possible changes in the availability of krill to the fishery. Currently, most fishing activities occur around the AP and southern Scotia Sea (Subareas 48.1 and 48.2, respectively)<sup>49</sup>. During recent years, the fishery around the AP usually reaches its catch limits in the middle of the fishing season (mid-autumn)<sup>50</sup>, triggering a management rule to move to a different spatial unit. Projected regional changes in RGGP—an increase in spring and decline in summer and autumn—may lead to shifts in the distribution and timing of fishing effort.

A southward shift in krill habitat will also have consequences for dependent predators. Species that are highly mobile and able to track changes in prey distribution may be less impacted than those that are tied to land-based colonies with restricted foraging ranges. This is especially relevant for predators breeding on sub-Antarctic islands, which rely on krill availability in low-mid latitudes<sup>11,51–54</sup>. South Georgia, for example, has a krill-dominated marine food web<sup>53,55</sup>, and our results suggest a decline in RGGP in this region. While CMIP5 models do not resolve mesoscale processes that are likely important to PP around South Georgia, even a high-PP future scenario also produced declines in RGGP at low latitudes<sup>10</sup>. Yet RGGP cannot be directly translated into changes in prey availability as it is a measure of relative habitat quality. RGGP is generally related to krill density, but this relationship is complex and contains caveats<sup>11,31</sup>. Methods for developing explicit projections of krill biomass are therefore needed for accurate predictions of impacts on predators.

Future krill habitat projections can build on our method in several ways. A growth model validated with in situ data from all seasons (not only summer) would be valuable<sup>21</sup>, and there is potential to use a more biologically realistic carbon-based krill growth model<sup>56</sup>. The life cycle of krill is complex, with different habitats used at different life-history stages<sup>25,57,58</sup>, and habitat quality in autumn–winter is considered of key importance in determining larval survival and juvenile recruitment<sup>58–61</sup>. Sea ice is thought to play a crucial role<sup>25,57,58</sup>, serving as an overwintering habitat for larval krill<sup>62,63</sup> and supplying an important food source via sea-ice biota<sup>64,65</sup>. Krill recruitment and abundance have both been linked to sea-ice extent<sup>14,59,66</sup>, with the latter projected to decrease about 25% by 2100<sup>67</sup>. However, while sea-ice extent is projected to decline,

observational and modelling studies examining other favourable ice characteristics (for example, optimal thickness to promote light for sea-ice algae<sup>68</sup>; sea-ice ridging to provide refuge<sup>63</sup>) have found that future habitat may expand<sup>62,69</sup>.

Our study provides a robust and quantitative assessment of future habitat quality, using a temperature- and food-related growth model that was empirically derived for krill sampled in the 20–60 mm length range. This provides a habitat quality estimate of individuals already recruited into the population. Since key knowledge gaps currently preclude a holistic quantitative assessment (incorporating sea ice or multiple other drivers such as ocean acidification<sup>7,70–73</sup>) there is a clear need for developing our largely qualitative understanding of sea-ice impacts on recruitment into quantitative relationships. Trait-based modelling<sup>9,74</sup> of the complete life cycle is one feasible approach to connect impacts on early life stages with growth and population dynamics.

In conclusion, our findings are relevant to the conservation of a globally important ecosystem and the management of the Southern Ocean's largest fishery. They provide an important step in developing the capacity to quantify climate change impacts on Southern Ocean ecosystems and outlines pathways to address key uncertainties.

## Online content

Any methods, additional references, Nature Research reporting summaries, source data, extended data, supplementary information, acknowledgements, peer review information; details of author contributions and competing interests; and statements of data and code availability are available at <https://doi.org/10.1038/s41558-020-0758-4>.

Received: 23 August 2019; Accepted: 20 March 2020;

Published online: 18 May 2020

## References

- Murphy, E. J. et al. Climatically driven fluctuations in Southern Ocean ecosystems. *Proc. R. Soc. Lond. B* **274**, 3057–3067 (2017).
- Murphy, E. J. et al. Understanding the structure and functioning of polar pelagic ecosystems to predict the impacts of change. *Proc. R. Soc. Lond. B* **283**, 20161646 (2016).
- Schmidt, K. et al. Seabed foraging by Antarctic krill: implications for stock assessment, benthopelagic coupling, and the vertical transfer of iron. *Limnol. Oceanogr.* **56**, 1411–1428 (2011).
- Trathan, P. N. & Hill, S. L. in *Biology and Ecology of Antarctic Krill* (ed. Volker, S.) 321–350 (Springer, 2016).
- Nicol, S., Foster, J. & Kawaguchi, S. The fishery for Antarctic krill—recent developments. *Fish Fish.* **13**, 30–40 (2011).
- Nicol, S. & Foster, J. in *Biology and Ecology of Antarctic Krill* (ed. Volker, S.) 387–421 (Springer, 2016).
- Flores, H. et al. Impact of climate change on Antarctic krill. *Mar. Ecol. Prog. Ser.* **458**, 1–19 (2012).
- McBride, M. M. et al. Krill, climate, and contrasting future scenarios for Arctic and Antarctic fisheries. *ICES J. Mar. Sci.* **71**, 1934–1955 (2014).
- Constable, A. J. et al. Climate change and Southern Ocean ecosystems I: how changes in physical habitats directly affect marine biota. *Glob. Change Biol.* **20**, 3004–3025 (2014).
- Hill, S. L., Phillips, T. & Atkinson, A. Potential climate change effects on the habitat of Antarctic krill in the Weddell quadrant of the Southern Ocean. *PLoS ONE* **8**, e72246 (2013).
- Murphy, E. J. et al. Restricted regions of enhanced growth of Antarctic krill in the circumpolar Southern Ocean. *Sci. Rep.* **7**, 6963 (2017).
- Vaughan, D. G. et al. Recent rapid regional climate warming on the Antarctic Peninsula. *Climatic Change* **60**, 243–274 (2003).
- Meredith, M. et al. in *IPCC Special Report on the Ocean and Cryosphere in a Changing Climate* (eds Pörtner, H.-O. et al.) Ch. 3 (2019).
- Atkinson, A., Siegel, V., Pakhomov, E. & Rothery, P. Long-term decline in krill stock and increase in salps within the Southern Ocean. *Nature* **432**, 100–103 (2004).
- Loeb, V. J. & Santora, J. A. Climate variability and spatiotemporal dynamics of five Southern Ocean krill species. *Prog. Oceanogr.* **134**, 93–122 (2015).
- Cox, M. J. et al. No evidence for a decline in the density of Antarctic krill *Euphausia superba* Dana, 1850, in the Southwest Atlantic sector between 1976 and 2016. *J. Crust. Biol.* **38**, 656–661 (2018).
- Atkinson, A. et al. Krill (*Euphausia superba*) distribution contracts southward during rapid regional warming. *Nat. Clim. Change* **9**, 142–147 (2019).
- Hill, S. L., Atkinson, A., Pakhomov, E. A. & Siegel, V. Evidence for a decline in the population density of Antarctic krill *Euphausia superba* Dana, 1850 still stands. A comment on Cox et al. *J. Crust. Biol.* **39**, 316–322 (2019).
- Ross, R. M., Quetin, L. B., Baker, K. S., Vernet, M. & Smith, R. C. Growth limitation in young *Euphausia superba* under field conditions. *Limnol. Oceanogr.* **45**, 31–43 (2000).
- Kawaguchi, S., Candy, S. G., King, R., Naganobu, M. & Nicol, S. Modelling growth of Antarctic krill. I. Growth trends with sex, length, season, and region. *Mar. Ecol. Prog. Ser.* **306**, 1–15 (2006).
- Atkinson, A. et al. Natural growth rates in Antarctic krill (*Euphausia superba*): II. Predictive models based on food, temperature, body length, sex, and maturity stage. *Limnol. Oceanogr.* **51**, 973–987 (2006).
- Flato, G. et al. in *Climate Change 2013: The Physical Science Basis* (eds Stocker, T. F. et al.) 741–866 (Cambridge Univ. Press, 2013).
- Stock, C. A. et al. On the use of IPCC-class models to assess the impact of climate on Living Marine Resources. *Prog. Oceanogr.* **88**, 1–27 (2011).
- Flato, G. M. Earth system models: an overview. *WIREs Clim. Change* **2**, 783–800 (2011).
- Piñones, A. & Fedorov, A. V. Projected changes of Antarctic krill habitat by the end of the 21st century. *Geophys. Res. Lett.* **43**, 8580–8589 (2016).
- Leung, S., Cabré, A. & Marinov, I. A latitudinally banded phytoplankton response to 21st century climate change in the Southern Ocean across the CMIP5 model suite. *Biogeosciences* **12**, 5715–5734 (2015).
- Groeneveld, J. et al. How biological clocks and changing environmental conditions determine local population growth and species distribution in Antarctic krill (*Euphausia superba*): a conceptual model. *Ecol. Model.* **303**, 78–86 (2015).
- Höring, F., Teschke, M., Suberg, L., Kawaguchi, S. & Meyer, B. Light regime affects the seasonal cycle of Antarctic krill (*Euphausia superba*): impacts on growth, feeding, lipid metabolism, and maturity. *Can. J. Zool.* **96**, 1203–1213 (2018).
- Piccolin, F. et al. The seasonal metabolic activity cycle of Antarctic krill (*Euphausia superba*): evidence for a role of photoperiod in the regulation of endogenous rhythmicity. *Front. Physiol.* **9**, 1715 (2018).
- Quetin, L. B., Ross, R. M., Fritsen, C. H. & Vernet, M. Ecological responses of Antarctic krill to environmental variability: can we predict the future? *Antarct. Sci.* **19**, 253–266 (2007).
- Atkinson, A. et al. Oceanic circumpolar habitats of Antarctic krill. *Mar. Ecol. Prog. Ser.* **362**, 1–23 (2008).
- Atkinson, A., Siegel, V., Pakhomov, E., Jessopp, M. & Loeb, V. A re-appraisal of the total biomass and annual production of Antarctic krill. *Deep Sea Res. Part I* **56**, 727–740 (2009).
- Cavanagh, R. D. et al. A synergistic approach for evaluating climate model output for ecological applications. *Front. Mar. Sci.* **4**, 308 (2017).
- Turner, J., Bracegirdle, T. J., Phillips, T., Marshall, G. J. & Hosking, J. S. An initial assessment of Antarctic sea ice extent in the CMIP5 models. *J. Clim.* **26**, 1473–1484 (2013).
- Siegel, V. & Watkins, J. L. in *Biology and Ecology of Antarctic Krill* (ed. Siegel, V.) 21–100 (Springer, 2016).
- Meyer, B. & Teschke, M. in *Biology and Ecology of Antarctic Krill* (ed. Siegel, V.) 145–174 (Springer, 2016).
- Perry, F. A. et al. Habitat partitioning in Antarctic krill: spawning hotspots and nursery areas. *PLoS ONE* **14**, e0219325 (2019).
- Kawaguchi, S. in *Biology and Ecology of Antarctic Krill* (ed. Siegel, V.) 225–246 (Springer, 2016).
- Tarling, G. et al. Recruitment of Antarctic krill *Euphausia superba* in the South Georgia region: adult fecundity and the fate of larvae. *Mar. Ecol. Prog. Ser.* **331**, 161–179 (2007).
- Meijers, A. J. et al. Representation of the Antarctic Circumpolar Current in the CMIP5 climate models and future changes under warming scenarios. *J. Geophys. Res. Oceans* **117**, C12008 (2012).
- Heuzé, C., Heywood, K. J., Stevens, D. P. & Ridley, J. K. Southern Ocean bottom water characteristics in CMIP5 models. *Geophys. Res. Lett.* **40**, 1409–1414 (2013).
- Heywood, K. J. et al. Ocean processes at the Antarctic continental slope. *Phil. Trans. A* **372**, 20130047 (2014).
- Quetin, L. B. & Ross, R. M. Episodic recruitment in Antarctic krill *Euphausia superba* in the Palmer LTER study region. *Mar. Ecol. Prog. Ser.* **259**, 185–200 (2003).
- Saba, G. K. et al. Winter and spring controls on the summer food web of the coastal West Antarctic Peninsula. *Nat. Commun.* **5**, 4318 (2014).
- Turner, J. et al. Antarctic climate change and the environment: an update. *Polar Rec.* **50**, 237–259 (2013).
- Cai, W. et al. Increasing frequency of extreme El Niño events due to greenhouse warming. *Nat. Clim. Change* **4**, 111–116 (2014).

48. Murphy, E. J., Clarke, A., Abram, N. J. & Turner, J. Variability of sea-ice in the northern Weddell Sea during the 20th century. *J. Geophys. Res. Oceans* **119**, 4549–4572 (2014).
49. Report of the Thirty-seventh Meeting of the Scientific Committee (CCAMLR, 2018).
50. Krill Fishery Report 2018 (CCAMLR, 2018).
51. Reisinger, R. R. et al. Habitat modelling of tracking data from multiple marine predators identifies important areas in the Southern Indian Ocean. *Divers. Distrib.* **24**, 535–550 (2018).
52. Hindell, M. A. et al. in *The Kerguelen Plateau: Marine Ecosystem and Fisheries* (eds Duhamel, G. & Welsford, D.) 203–215 (Societe Francaise d'Ichtyologie, 2011).
53. Croxall, J. P., Reid, K. & Prince, P. A. Diet, provisioning and productivity responses of marine predators to differences in availability of Antarctic krill. *Mar. Ecol. Prog. Ser.* **177**, 115–131 (1999).
54. Goedegebuure, M. *Improving Representations of Higher Trophic-Level Species in Models: Using Individual-Based Modelling and Dynamic Energy Budget Theory to Project Population Trajectories of Southern Elephant Seals*. PhD thesis, University of Tasmania (2018).
55. Murphy, E. et al. Spatial and temporal operation of the Scotia Sea ecosystem: a review of large-scale links in a krill centred food web. *Phil. Trans. R. Soc. Lond. B* **362**, 113–148 (2007).
56. Constable, A. J. & Kawaguchi, S. Modelling growth and reproduction of Antarctic krill, *Euphausia superba*, based on temperature, food and resource allocation amongst life history functions. *ICES J. Mar. Sci.* **75**, 738–750 (2017).
57. Nicol, S. Krill, currents, and sea ice: *Euphausia superba* and its changing environment. *Bioscience* **56**, 111–120 (2006).
58. Thorpe, S. E., Tarling, G. A. & Murphy, E. J. Circumpolar patterns in Antarctic krill larval recruitment: an environmentally driven model. *Mar. Ecol. Prog. Ser.* **613**, 77–96 (2019).
59. Siegel, V. & Loeb, V. Recruitment of Antarctic krill *Euphausia superba* and possible causes for its variability. *Mar. Ecol. Prog. Ser.* **123**, 45–56 (1995).
60. Lowe, A. T., Ross, R. M., Quetin, L. B., Vernet, M. & Fritsen, C. H. Simulating larval Antarctic krill growth and condition factor during fall and winter in response to environmental variability. *Mar. Ecol. Prog. Ser.* **452**, 27–43 (2012).
61. Yoshida, T. et al. Structural changes in the digestive glands of larval Antarctic krill (*Euphausia superba*) during starvation. *Polar Biol.* **32**, 503–507 (2009).
62. Meyer, B. et al. The winter pack-ice zone provides a sheltered but food-poor habitat for larval Antarctic krill. *Nat. Ecol. Evol.* **1**, 1853–1861 (2017).
63. Meyer, B. et al. Physiology, growth, and development of larval krill *Euphausia superba* in autumn and winter in the Lazarev Sea, Antarctica. *Limnol. Oceanogr.* **54**, 1595–1614 (2009).
64. Kohlbach, D. et al. Ice algae-produced carbon is critical for overwintering of Antarctic krill *Euphausia superba*. *Front. Mar. Sci.* **4**, 310 (2017).
65. Meyer, B. The overwintering of Antarctic krill, *Euphausia superba*, from an ecophysiological perspective. *Polar Biol.* **35**, 15–37 (2012).
66. Mackintosh, N. A. Life cycle of Antarctic krill in relation to ice and water conditions. *Discovery Rep.* **36**, 1–94 (1972).
67. Arzel, O., Fichefet, T. & Goosse, H. Sea ice evolution over the 20th and 21st centuries as simulated by current AOGCMs. *Ocean Model. Online* **12**, 401–415 (2006).
68. Meiners, K. et al. Chlorophyll *a* in Antarctic sea ice from historical ice core data. *Geophys. Res. Lett.* **39**, L21602 (2012).
69. Melbourne-Thomas, J. et al. Under ice habitats for Antarctic krill larvae: could less mean more under climate warming? *Geophys. Res. Lett.* **43**, 10322–10327 (2016).
70. Kawaguchi, S. et al. Risk maps for Antarctic krill under projected Southern Ocean acidification. *Nat. Clim. Change* **3**, 843–847 (2013).
71. Ericson, J. A. et al. Adult Antarctic krill proves resilient in a simulated high CO<sub>2</sub> ocean. *Commun. Biol.* **1**, 190 (2018).
72. Riebesell, U. et al. Enhanced biological carbon consumption in a high CO<sub>2</sub> ocean. *Nature* **450**, 545–548 (2007).
73. Cummings, V. J. et al. In situ response of Antarctic under-ice primary producers to experimentally altered pH. *Sci. Rep.* **9**, 6069 (2019).
74. Renaud, P. E. et al. Pelagic food-webs in a changing Arctic: a trait-based perspective suggests a mode of resilience. *ICES J. Mar. Sci.* **75**, 1871–1881 (2018).
75. SeaWiFS Level-3 Binned Chlorophyll Data version 2018 (NASA OB.DAAC, 2018); 10.5067/ORBVIEW-2/SEAWIFS/L3B/CHL/2018
76. Johnson, R., Strutton, P. G., Wright, S. W., McMinn, A. & Meiners, K. M. Three improved satellite chlorophyll algorithms for the Southern Ocean. *J. Geophys. Res. Oceans* **118**, 3694–3703 (2013).
77. Orsi, A. H., Whitworth III, T. & Nowlin Jr, W. D. On the meridional extent and fronts of the Antarctic Circumpolar Current. *Deep Sea Res. Part I* **42**, 641–673 (1995).
78. Sumner, M. D. *raadtools: Tools for Synoptic Environmental Spatial Data*. R package version 0.5.3.9001 (2020).

**Publisher's note** Springer Nature remains neutral with regard to jurisdictional claims in published maps and institutional affiliations.

© The Author(s), under exclusive licence to Springer Nature Limited 2020

## Methods

Circumpolar growth potential calculated from an ensemble of available CMIP5 ESMs was assessed against observation-based growth potential using seasonal Taylor diagrams. This assessment produced a weighted model subset with greater skill at reproducing krill growth. This weighted subset was then applied to future projections for two IPCC climate change scenarios, or RCPs: 4.5, where climate policy works to reduce emissions and radiative forcing stabilized shortly after 2100, and 8.5, a ‘business as usual scenario’ where emissions continue to rise on their current trajectories<sup>79</sup>. All analyses were performed in the R statistical computing environment<sup>80</sup>.

**Krill growth potential and biomass models.** To model seasonal growth potential using ESM outputs, we built on a previous study that modelled current growth potential from satellite observations<sup>11</sup>. The following empirical model deriving daily growth rate (DGR, mm d<sup>-1</sup>), in which  $a$ – $g$  represent constants derived from the empirical model, was used<sup>21</sup>:

$$\text{DGR} = a + b \times \text{Length} + c \times \text{Length}^2 + \left[ d \times \frac{\text{chlorophyll}}{e + \text{chlorophyll}} \right] + f \times \text{SST} + g \times \text{SST}^2 + \text{error} \quad (1)$$

The in situ data originally used to develop the empirical growth model<sup>21</sup> represent only one region within the circumpolar range of krill, for one season (summer, a season of high growth rates for krill) and within a specific temperature range ( $-1$  to  $5^\circ\text{C}$ ). As data on krill growth outside of these conditions are sparse, it is uncertain whether we can reliably extrapolate these calculations as actual growth values. A recent study<sup>19</sup> has shown that within the same season and temperature limits, the growth model produces realistic circumpolar krill growth habitat distributions. This precedent allows us to reasonably assume that these relationships will hold in general. We consider daily growth rate to thus more accurately represent growth potential, a measure of habitat quality that can be used for comparative purposes.

All growth potential calculations were done using seasonal climatologies of SST and surface chlorophyll. The empirical growth model was derived over an SST range between  $-1$  and  $5^\circ\text{C}$ ; hence, temperatures above this maximum were masked. However, after examining krill growth predictions based on historical satellite observations, we concluded that limiting SST to above  $-1^\circ\text{C}$  excluded regions in the southern Ross Sea in summer, which are likely important whale foraging areas for krill<sup>35,81</sup>. Therefore, we accepted regions with SST  $<-1^\circ\text{C}$  with the caveat that projections for SST below this threshold have increased uncertainty. The  $-1^\circ\text{C}$  SST contour is presented on maps to identify these areas. For each cell, if SST was present and chlorophyll was absent, then chlorophyll was set to  $0\text{ mg m}^{-3}$ , whereas if there was sea-ice cover, the cell was excluded from the calculation.

To calculate seasonal growth potential in mm month<sup>-1</sup>, we assumed an individual krill with a starting length of 40 mm, the observed mean length of adult krill<sup>3</sup>. Although previous analyses have included other starting size classes<sup>10,11</sup>, we found that projected differences between future and historical epochs remained the same irrespective of starting length. For each day in the season, DGR was calculated using the SST and chlorophyll fields and then added to the previous length.

Growth potential, a metric based on length, was translated into gross growth potential (GGP), a metric based on biomass. Biomass is more relevant when interpreting impacts on dependant predators and the fishery, as it translates directly into the amount of energy consumed by a predator or fishery yield. Since seasonal growth potential was presented as a monthly value, GGP for a season is defined here as the dry mass of an individual krill at the end of a month in a season divided by the beginning of the month in that season. It therefore represents the proportional change in dry mass, with a value of 1 indicating that GGP remains constant. Krill length (mm), derived using equation (1), was converted to dry mass (mg) using the following relationship<sup>10</sup>:

$$\log_{10}(\text{Mass}) = 3.89 \log_{10}(\text{Length}) - 4.19 \quad (2)$$

**SST and chlorophyll fields.** Using equation (1), seasonal surface averages of growth were calculated for the observation-based and model-based SST and chlorophyll fields summarized in Supplementary Table 1.

Seasonal surface averages of satellite observation-based datasets for SST and chlorophyll, taken over the period of December 1997 to December 2010 for the Southern Ocean (south of  $50^\circ\text{S}$ ) were accessed using the raadtools package<sup>78</sup>. For SST, the Optimum Interpolation SST (OISST) v2 daily dataset (1/4° horizontal resolution) was used. For chlorophyll, the daily datasets (1/12° horizontal resolution) for both the original SeaWiFS<sup>75</sup> and the Johnson et al.<sup>76</sup> corrected estimate of SeaWiFS were used. To calculate growth potential, the OISST dataset was sampled to match the higher-resolution chlorophyll datasets using bilinear interpolation. Although the Johnson et al.<sup>76</sup> dataset is likely a more accurate approximation of surface phytoplankton biomass<sup>76</sup>, we elected to average the two chlorophyll datasets when calculating observation-based growth potential to explicitly acknowledge that satellite observations approximate truth with varying

degrees of error (Extended Data Fig. 7). By incorporating two different algorithms, the latter of which is tuned to in situ chlorophyll estimates taken from the Southern Ocean, we represent the variability surrounding our observation-based benchmark (Extended Data Fig. 3).

ESMs used in this analysis included one ensemble member from most models in the CMIP5 archive that contributed sea surface temperature (tos in the IPCC shorthand) and chlorophyll (chl), as well as the Norwegian Earth System Model (medium resolution, NorESM1-ME), which contributed phyc (a carbon-based analogue of chl)<sup>82</sup>. In line with the calculation used with NorESM1-ME, this was converted to chlorophyll using a constant carbon/chlorophyll ratio of 60<sup>82</sup> (J.F. Tjiputra, personal communication). Growth potential was evaluated for two different IPCC climatologies: ‘historical’ (1960–1989), which represents current climate, and ‘future’ (2070–2099). This latter climatology was calculated for two RCPs: RCP 4.5 and RCP 8.5.

**Weighted subset selection.** The weighted model subset was determined by evaluating the ability of each model to reproduce observation-based growth potential for current climate conditions. For models, current climate was represented by averaging seasonal outputs over 1960–1989. To allow direct comparison, bilinear interpolation was used to re-grid the (11) model-based seasonal surface averages for growth potential onto the same  $1^\circ \times 1^\circ$  grid. These models were compared with observation-based growth potential, also resampled to the same grid, using a seasonally split Taylor diagram (Fig. 1).

We excluded models that had a normalized standard deviation  $>\pm 0.5$  of observation-based growth potential and a correlation  $<0.1$ . Of the models that remained, the Geophysical Fluid Dynamics Laboratory’s Earth System models GFDL-ESM2G and GFDL-ESM2M (2G and 2M, respectively) were contributed by the same institution<sup>83,84</sup>. They differed only in their physical ocean component and thus were not independent<sup>83</sup>. To avoid pseudoreplication, there were two options: remove one of the models from the analysis or weight them each as half. The Taylor diagram shows that apart from standard deviation in spring, 2M more closely approaches observed standard deviation and has higher correlation to observed growth potential than 2G. Since the 2G model did not perform as well as 2M in most instances, the first option was chosen and 2G was removed from the analysis.

To weight the remaining models, five different weighting schemes were trialled (Extended Data Fig. 4):

$$\begin{aligned} \text{Weightingscheme1} &= \frac{1}{x} \\ \text{Weightingscheme2} &= e^{-x(\frac{x}{0.1^2})} \\ \text{Weightingscheme3} &= e^{-x(\frac{x}{0.15^2})} \\ \text{Weightingscheme4} &= e^{-x(\frac{x}{0.2^2})} \\ \text{Weightingscheme5} &= e^{-x(\frac{x}{0.25^2})} \end{aligned}$$

where  $x$  is the standard deviation of the model (mm month<sup>-1</sup>) under consideration ( $\text{s.d.}_{\text{mod}}$ ), as calculated for the growth potential Taylor diagram in Fig. 1. For the purposes of comparison, if  $\text{s.d.}_{\text{mod}} > 1$ , then the value was reflected about the  $\text{s.d.} = 1$  axis by subtracting it from 2.

Overall, we found that regardless of the specific weighting scheme, if models with a standard deviation closer to observed were given higher weight, then the results were robust (Extended Data Fig. 5). The greatest variation between weighting schemes occurred in autumn, which was due to observed standard deviation being represented by a small proportion of the models (Fig. 1). To select a weighting scheme, we again referenced a Taylor diagram that evaluated weighting scheme performance at reproducing growth potential against observations (Extended Data Fig. 6). Since the greatest variation between schemes occurred in autumn, we narrowed our choice to the two schemes with standard deviations closest to 1: weighting schemes 3 and 4. Of these, weighting scheme 4 was selected, as weighting scheme 3 greatly overestimated growth potential in the Weddell, Amundsen and eastern Ross seas.

**Future projections.** Future projections from the weighted subset were used to calculate a weighted multimodel mean of seasonal krill growth potential for the RCP scenarios 4.5 and 8.5. This was then implemented using equation (2) to calculate GGP. The relative change between historical and future GGP is represented in this study as RGGP.

**Reporting Summary.** Further information on research design is available in the Nature Research Reporting Summary linked to this article.

## Data availability

The data that support the findings of this study are publicly available at the Australian Antarctic Data Centre, <https://doi.org/10.26179/p2e4-5695> (ref. 85). The CMIP5 output is available from the Earth System Grid Federation (<https://esgf-node.llnl.gov/projects/cmip5/>). In addition to being retrievable using the raadtools package in R (<https://github.com/AustralianAntarcticDivision/raadtools>), the satellite data can be found at <https://www.ncei.noaa.gov/metadata/geoportal/rest/metadata/item/gov.noaa.ncdc:C00844/html> for sea surface temperature, <https://oceancolor.gsfc.nasa.gov/data/seawifs/> for SeaWiFS<sup>75</sup> chlorophyll *a* and [https://data.aad.gov.au/metadata/records/AAS\\_4343\\_so\\_chlorophyll](https://data.aad.gov.au/metadata/records/AAS_4343_so_chlorophyll) for the Johnson et al.<sup>76</sup> chlorophyll *a* data.

## Code availability

The code relating to this study is available from the corresponding author on request.

## References

79. van Vuuren, D. P. et al. The representative concentration pathways: an overview. *Climatic Change* **109**, 5–31 (2011).
80. R Core Team *R: A Language and Environment for Statistical Computing* (R Foundation for Statistical Computing, 2018).
81. Riekkola, L. et al. Application of a multi-disciplinary approach to reveal population structure and Southern Ocean feeding grounds of humpback whales. *Ecol. Indic.* **89**, 455–465 (2018).
82. Tjiputra, J. F. et al. Evaluation of the carbon cycle components in the Norwegian Earth system model (NorESM). *Geosci. Model Dev.* **6**, 301–325 (2013).
83. Dunne, J. P. et al. GFDL's ESM2 global coupled climate–carbon Earth system models. Part I: physical formulation and baseline simulation characteristics. *J. Clim.* **25**, 6646–6665 (2012).
84. Dunne, J. P. et al. GFDL's ESM2 global coupled climate–carbon Earth system models. Part II: carbon system formulation and baseline simulation characteristics. *J. Clim.* **26**, 2247–2267 (2013).
85. Veytia, D. et al. *Circumpolar Projections of Antarctic Krill (Euphausia superba) Growth Potential* version 1 (Australian Antarctic Data Centre, 2020).

## Acknowledgements

We thank A. Constable, R. Johnson and A. Lenton for their advice on the project, as well as M. Sumner and J. Berkhouit for their technical support.

We acknowledge the World Climate Research Programme's Working Group on Coupled Modelling, which is responsible for CMIP, and we thank the climate modelling groups (listed in Supplementary Table 2) for producing and making available their model output. For CMIP, the US Department of Energy's Program for Climate Model Diagnosis

and Intercomparison provides coordinating support and led development of software infrastructure in partnership with the Global Organization for Earth System Science Portals.

This research was supported by the Australian Government through Antarctic Science Project 4408 and the Cooperative Research Centres Programme through the Antarctic Climate and Ecosystems Cooperative Research Centre (ACE CRC). D.V. is the recipient of a Tasmania Graduate Research Scholarship provided by the University of Tasmania. S.B. is the recipient of an Australian Research Council Australian Discovery Early Career Award (project DE180100828). E.M. was supported by the BAS ALI-Science Ecosystems project (developing krill life-cycle models and future projections) and acknowledges BAS colleagues for discussions on the development of analyses, models and projections of Antarctic krill population processes. The study is also a contribution to the international Integrating Climate and Ecosystems Dynamics Programme (ICED).

## Author contributions

The study was developed by all authors. All authors supervised D.V. in conducting the analyses, designing figures and preparing the manuscript, as well as provided feedback and ideas in the manuscript development.

## Competing interests

The authors declare no competing interests.

## Additional information

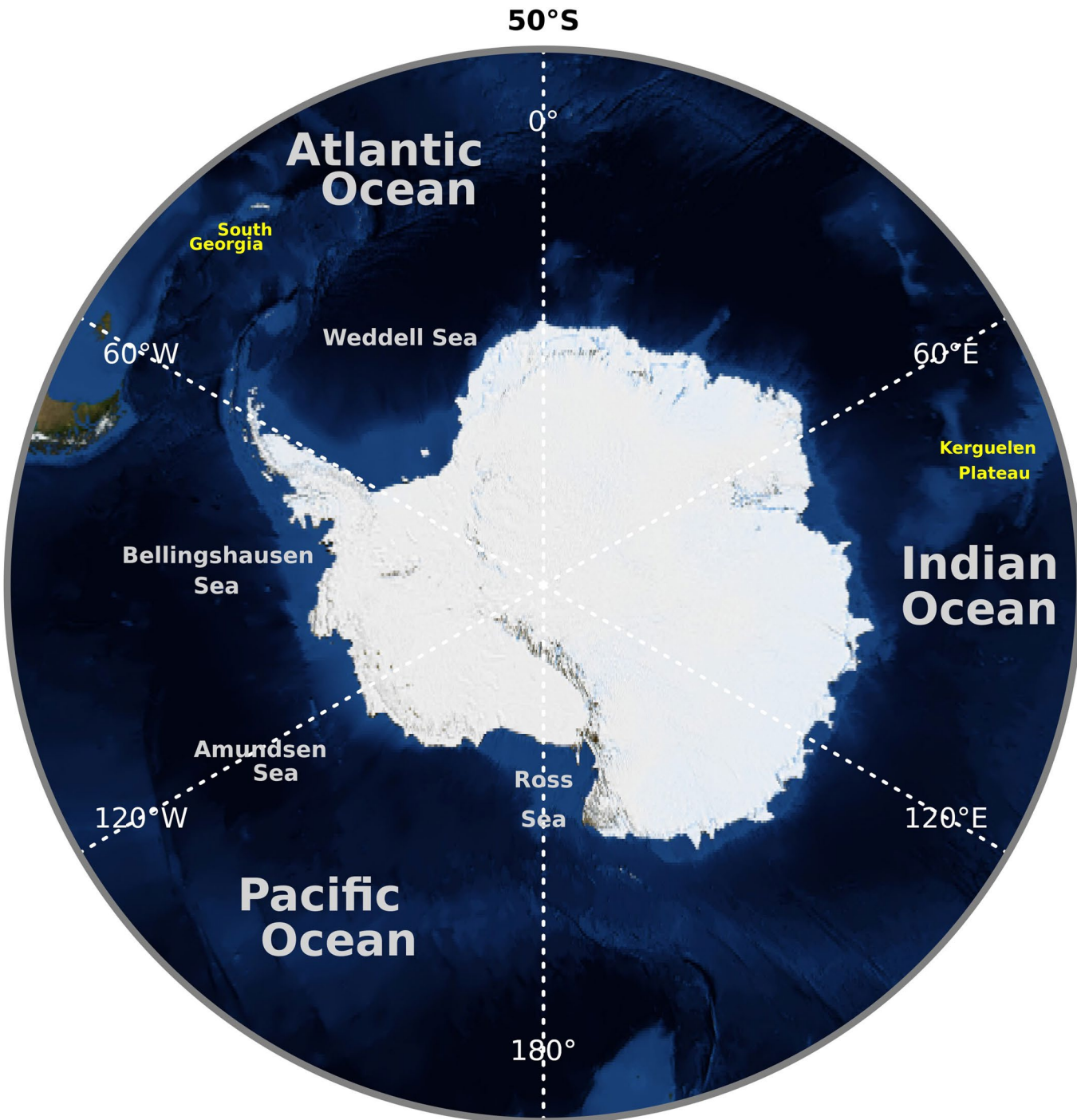
**Extended data** is available for this paper at <https://doi.org/10.1038/s41558-020-0758-4>.

**Supplementary information** is available for this paper at <https://doi.org/10.1038/s41558-020-0758-4>.

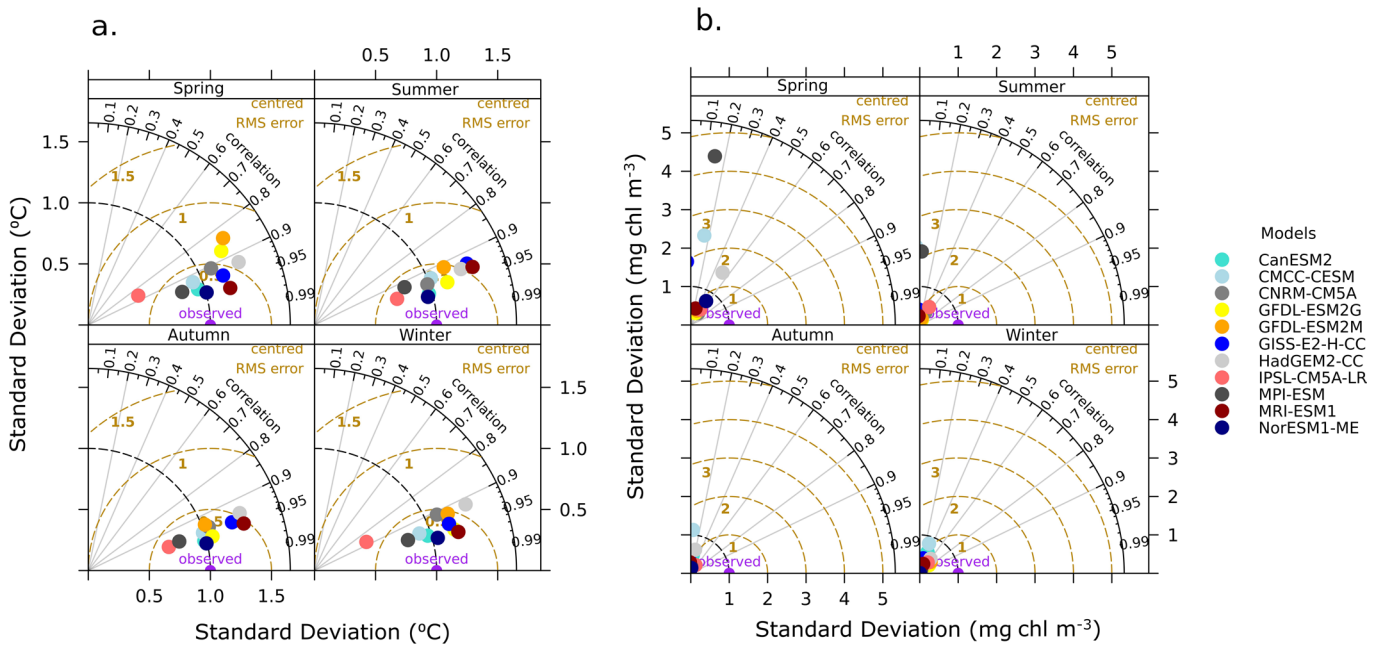
**Correspondence and requests for materials** should be addressed to D.V.

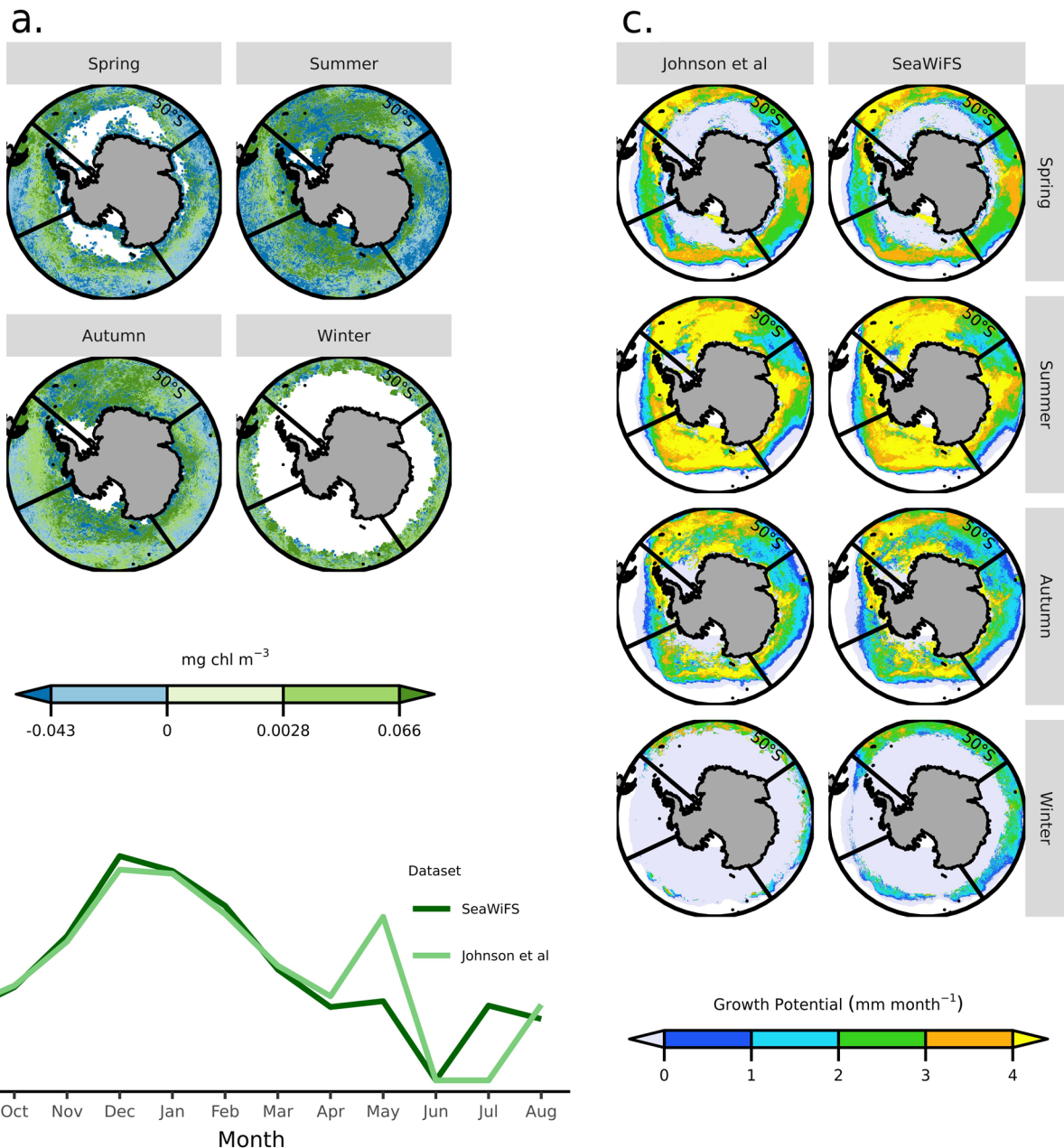
**Peer review information** *Nature Climate Change* thanks Jilda Caccavo, Bettina Fach and Elisa Ravagnan for their contribution to the peer review of this work.

**Reprints and permissions information** is available at [www.nature.com/reprints](http://www.nature.com/reprints).

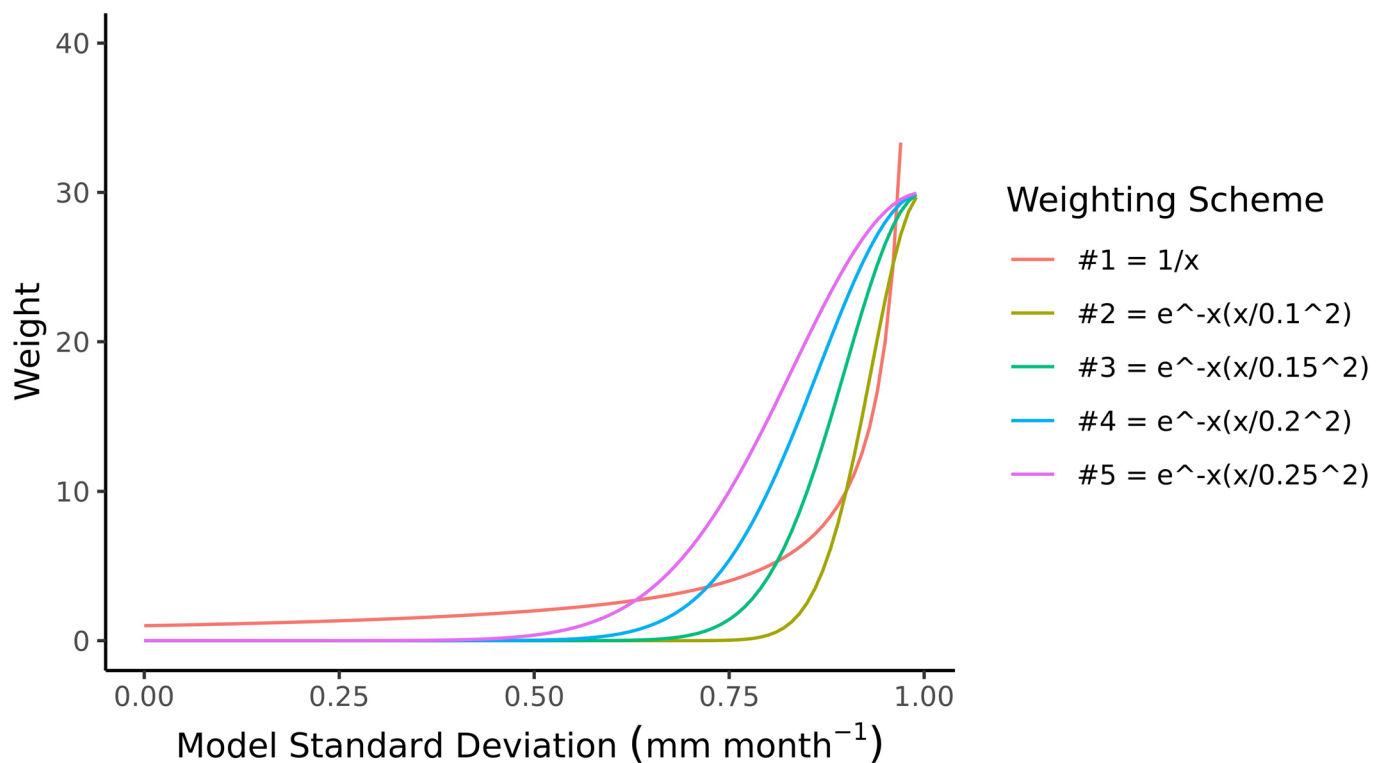


**Extended Data Fig. 1 | Map of study area.** Highlights commonly referenced locations throughout the text. White text with a large font size denotes ocean basins, white text with a small font size denotes seas, and yellow text denotes commonly-referenced topographic features.

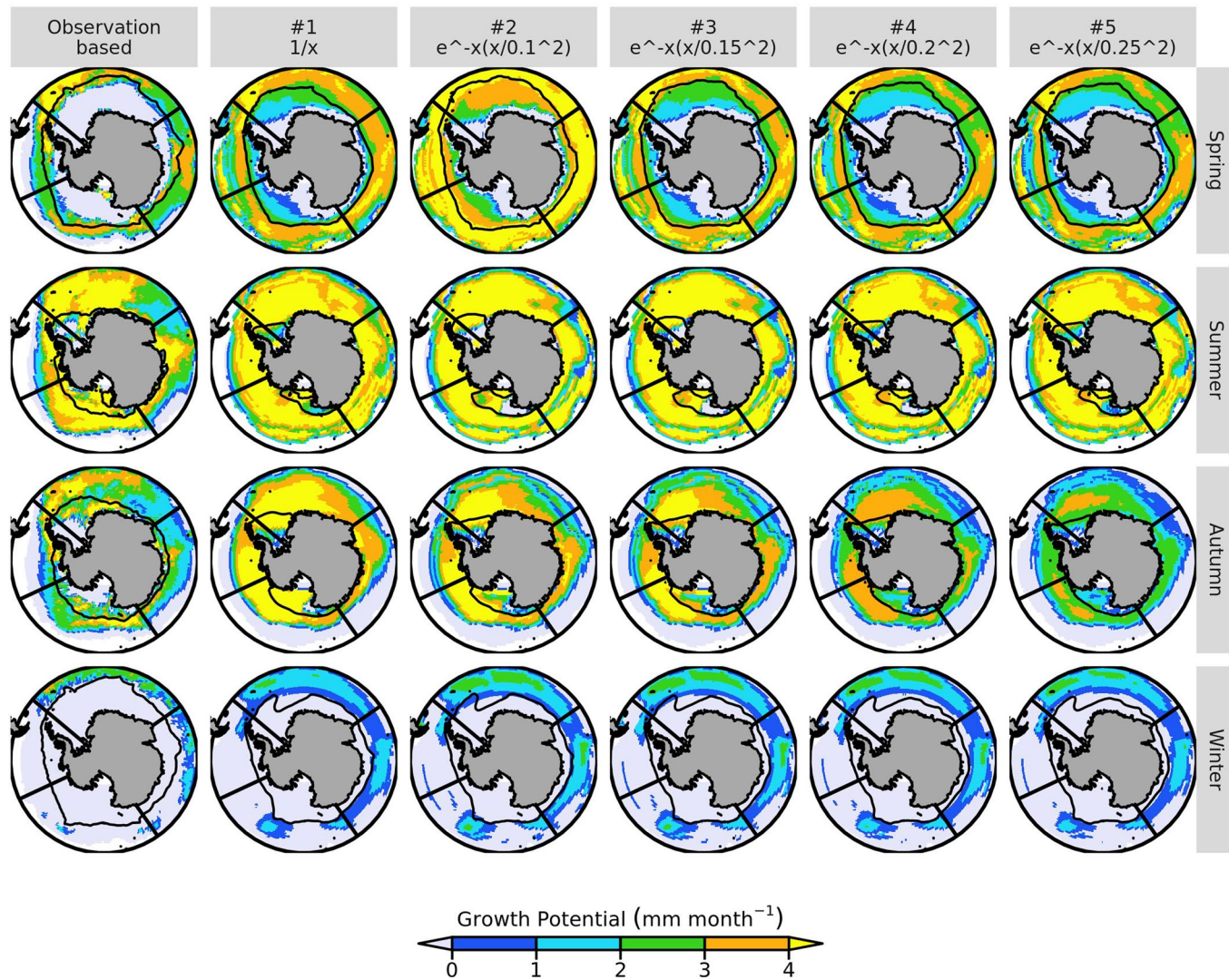




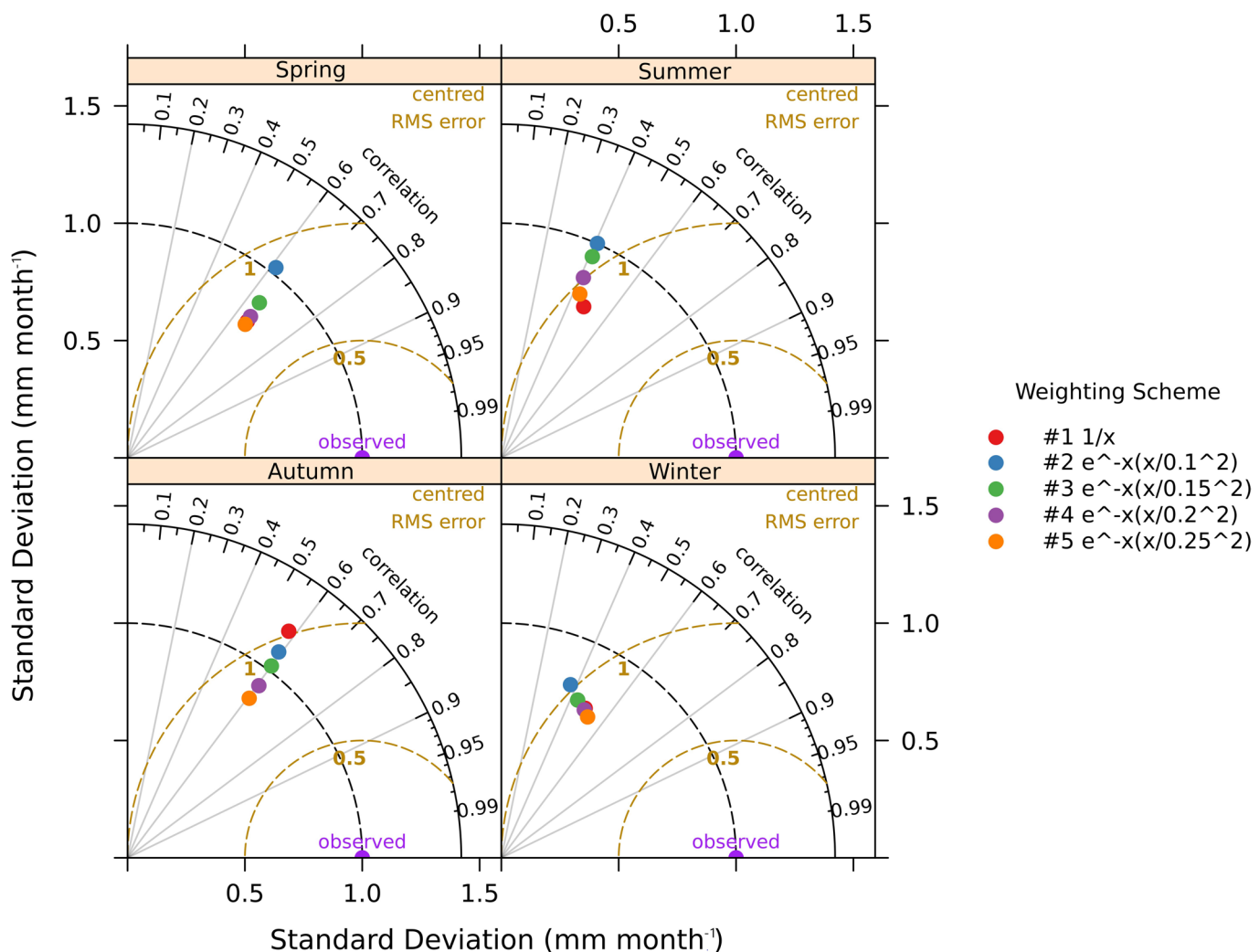
**Extended Data Fig. 3 | Comparing chlorophyll observation datasets.** These values represent a climatology taken from Dec 1997-2010. **a**, is the difference of seasonal surface averages of the Johnson et al.<sup>76</sup> dataset minus the SeaWiFS<sup>75</sup> dataset. **b**, The climatologies of the two datasets using a monthly timeseries. **c**, Seasonal growth potential calculated using each chlorophyll dataset and OISST v2 SST. Black meridional lines on maps delineate ocean basin sectors<sup>9</sup>.



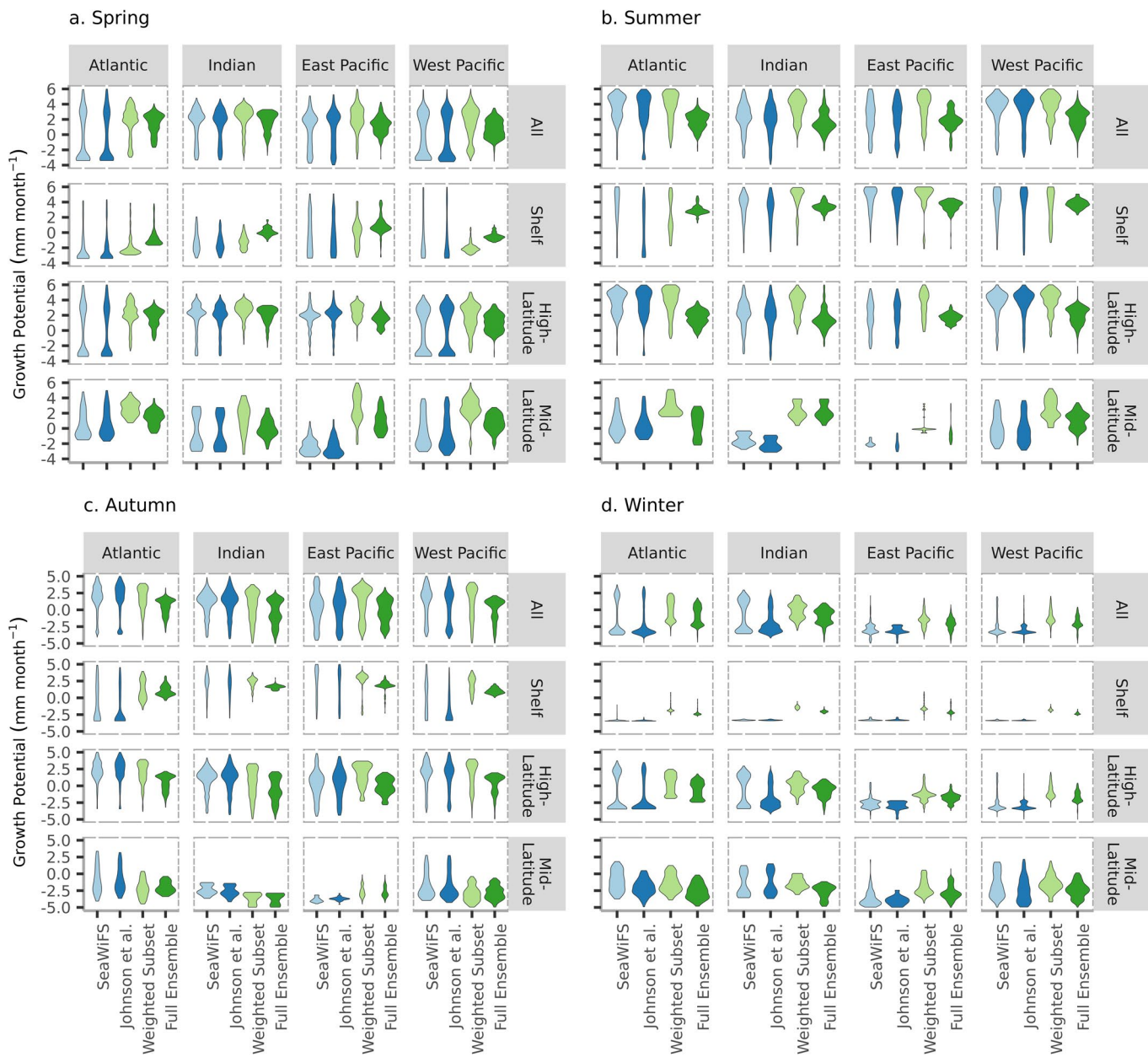
**Extended Data Fig. 4 | Different model weighting schemes trialled.** To compare the shapes of these weighting schemes together, weighting schemes #2-5 were multiplied by a constant of 30.



**Extended Data Fig. 5 | Observation-based seasonal growth potential compared to different model weighting schemes.** The five weighting schemes pictured correspond to the weighting schemes picture in Supplementary Fig. 3. Observation-based growth potential here represents the mean calculated from the Johnson et al.<sup>76</sup> and SeaWiFS<sup>75</sup> datasets pictured in Supplementary Fig. 2c. Growth potential for the model weighting schemes was calculated over the CMIP5 “historical” period of 1960–1989. Black meridional lines on maps delineate ocean basin sectors<sup>9</sup>.



**Extended Data Fig. 6 | Taylor diagram assessing modelled growth potential of different weighting schemes trialled.** The weighting schemes correspond to the weighting schemes picture in Supplementary Fig. 3, except that weighting schemes #2–5 were not multiplied by a constant of 30. Statistics for the Taylor diagram were calculated from the area-weighted seasonal modelled growth potential, averaged over 1960–1989. Observation-based growth potential was calculated using the average of the SeaWiFS<sup>75</sup> and Johnson et al.<sup>76</sup> chlorophyll datasets and the OISST v2 dataset, over the climatology of 1997–2010.



**Extended Data Fig. 7 | Comparing the density of growth potential values between chlorophyll datasets, the weighted subset and full ensemble.**

The growth potential values represented were taken from surface averages, for **a**, spring, **b**, summer, **c**, autumn and **d**, winter. Averages were taken over the period of Dec 1997-2010 for the chlorophyll datasets and 1960-1989 for models. See reference for definitions of the sectors and zones used<sup>9</sup>. The distribution of growth potential values from the weighted subset falls largely within the range of observed variability obtained using the two different Southern Ocean chlorophyll-a algorithms, particularly during spring and summer, which are the seasons with the greatest observation coverage.

# Reporting Summary

Nature Research wishes to improve the reproducibility of the work that we publish. This form provides structure for consistency and transparency in reporting. For further information on Nature Research policies, see [Authors & Referees](#) and the [Editorial Policy Checklist](#).

## Statistics

For all statistical analyses, confirm that the following items are present in the figure legend, table legend, main text, or Methods section.

n/a Confirmed

- The exact sample size ( $n$ ) for each experimental group/condition, given as a discrete number and unit of measurement
- A statement on whether measurements were taken from distinct samples or whether the same sample was measured repeatedly
- The statistical test(s) used AND whether they are one- or two-sided  
*Only common tests should be described solely by name; describe more complex techniques in the Methods section.*
- A description of all covariates tested
- A description of any assumptions or corrections, such as tests of normality and adjustment for multiple comparisons
- A full description of the statistical parameters including central tendency (e.g. means) or other basic estimates (e.g. regression coefficient) AND variation (e.g. standard deviation) or associated estimates of uncertainty (e.g. confidence intervals)
- For null hypothesis testing, the test statistic (e.g.  $F$ ,  $t$ ,  $r$ ) with confidence intervals, effect sizes, degrees of freedom and  $P$  value noted  
*Give P values as exact values whenever suitable.*
- For Bayesian analysis, information on the choice of priors and Markov chain Monte Carlo settings
- For hierarchical and complex designs, identification of the appropriate level for tests and full reporting of outcomes
- Estimates of effect sizes (e.g. Cohen's  $d$ , Pearson's  $r$ ), indicating how they were calculated

*Our web collection on [statistics for biologists](#) contains articles on many of the points above.*

## Software and code

Policy information about [availability of computer code](#)

Data collection

observation-based datasets were retrieved using the raadtools function in R (see Methods), and CMIP5 model output was retrieved from the National Computational Infrastructure (NCI).

Data analysis

All analyses were conducted in the R language and environment for statistical computing

For manuscripts utilizing custom algorithms or software that are central to the research but not yet described in published literature, software must be made available to editors/reviewers. We strongly encourage code deposition in a community repository (e.g. GitHub). See the Nature Research [guidelines for submitting code & software](#) for further information.

## Data

Policy information about [availability of data](#)

All manuscripts must include a [data availability statement](#). This statement should provide the following information, where applicable:

- Accession codes, unique identifiers, or web links for publicly available datasets
- A list of figures that have associated raw data
- A description of any restrictions on data availability

The data that support the findings of this study are publicly available at the Australian Antarctic Data Centre, DOI:10.26179/5e27c6584e0f8. The CMIP5 output is available from the Earth System Grid Federation (<https://esgf-node.llnl.gov/projects/cmip5/>). In addition to being retrievable using the raadtools package in R (<https://github.com/AustralianAntarcticDivision/raadtools>), the satellite data can also be found at (<https://www.ncei.noaa.gov/metadata/geoportal/rest/metadata/item/gov.noaa.ncdc:C00844/html>) for sea surface temperature, (<https://oceancolor.gsfc.nasa.gov/data/seawifs/>) for SeaWiFS chlorophyll-a, and ([https://data.aad.gov.au/metadata/records/AAS\\_4343\\_so\\_chlorophyll](https://data.aad.gov.au/metadata/records/AAS_4343_so_chlorophyll)) for the Johnson et al. chlorophyll-a data.

# Field-specific reporting

Please select the one below that is the best fit for your research. If you are not sure, read the appropriate sections before making your selection.

- Life sciences       Behavioural & social sciences       Ecological, evolutionary & environmental sciences

For a reference copy of the document with all sections, see [nature.com/documents/nr-reporting-summary-flat.pdf](https://nature.com/documents/nr-reporting-summary-flat.pdf)

## Ecological, evolutionary & environmental sciences study design

All studies must disclose on these points even when the disclosure is negative.

Study description

We assess future changes in krill habitat by forcing an empirical growth model with CMIP5 model projected seasonal climatologies of SST and chlorophyll-a for the historical (1960-1989) and future (2070-2099) periods.

Research sample

The krill growth model used came from an existing study. The model was empirically-derived, and modeled the effects of food, temperature and krill length on in situ summer growth of krill across the southwest Atlantic sector of the Southern Ocean from research cruises in the summers of 2002 and 2003 (see Atkinson et al., 2006). The remaining data used was either satellite observation-based datasets or climate model output. Any associated sampling information on the individual datasets is available through the provided links in the Data Availability Statement.

Sampling strategy

See referenced datasets and models

Data collection

See referenced datasets and models

Timing and spatial scale

See referenced datasets and models

Data exclusions

No data were excluded

Reproducibility

No experiments were conducted, accessing datasets is all that is required to reproduce results.

Randomization

See referenced datasets and models

Blinding

Blinding was not relevant, as models were evaluated using a quantitative approach, and thus experimenter bias was as limited as possible.

Did the study involve field work?  Yes  No

## Reporting for specific materials, systems and methods

We require information from authors about some types of materials, experimental systems and methods used in many studies. Here, indicate whether each material, system or method listed is relevant to your study. If you are not sure if a list item applies to your research, read the appropriate section before selecting a response.

Materials & experimental systems

- |                                     |  |
|-------------------------------------|--|
| n/a                                 | Involved in the study                                |
| <input checked="" type="checkbox"/> | <input type="checkbox"/> Antibodies                  |
| <input checked="" type="checkbox"/> | <input type="checkbox"/> Eukaryotic cell lines       |
| <input checked="" type="checkbox"/> | <input type="checkbox"/> Palaeontology               |
| <input checked="" type="checkbox"/> | <input type="checkbox"/> Animals and other organisms |
| <input checked="" type="checkbox"/> | <input type="checkbox"/> Human research participants |
| <input checked="" type="checkbox"/> | <input type="checkbox"/> Clinical data               |

Methods

- |                                     |   |
|-------------------------------------|---|
| n/a                                 | Involved in the study                           |
| <input checked="" type="checkbox"/> | <input type="checkbox"/> ChIP-seq               |
| <input checked="" type="checkbox"/> | <input type="checkbox"/> Flow cytometry         |
| <input checked="" type="checkbox"/> | <input type="checkbox"/> MRI-based neuroimaging |